Distance-based Formation Control of a Three-Robot System

Zhuo Chen, Chao Jiang, Yi Guo

Department of Electrical and Computer Engineering, Stevens Institute of Technology, Hoboken, NJ 07030, USA. E-mail: {zchen39,cjiang6,yguo1}@stevens.edu

Abstract: Distance-based formation control becomes popular since it does not require absolute positions to be sensed by each agent, which makes it suitable for vision-based robot formation control tasks. In this paper, we present a distributed control law for a group of three differential-drive robots to maintain a desired formation with a common desired velocity. As a first step, the control law for a group of three single-integrator modeled agents is presented and proved. Then, the control law is extended to a group of nonholonomic robots by using a coordinate transformation technique while considering the input saturation nonlinearity. Finally, the designed controller is verified in a robot simulator V-REP. Simulation results have shown that the control performance is satisfactory.

Key Words: Distance-based Formation Control, Differential Drive Robot, Input Saturation

1 Introduction

Multi-robot formation control has attracted a significant amount of research attentions in recent decades. According to [1], the problem of multi-agent formation control can be classified into position-, displacement- and distancebased formation control depending on the system's sensing capabilities and interaction topologies. Position-based formation control imposes the highest requirement on the system's sensing capability, where the absolute position of each agent with respect to a common global reference frame must be known. In comparison, displacement-based formation control uses only the local frame of each agent instead of a common global reference frame. Yet, the local reference frame used in the displacement-based formation control must have the same orientation. In contrast, the distance-based formation control eliminates the requirement of a common orientation between different agents, which makes it suitable for vision-based regulation and control of mobile robots [2-5], and also for cases where sensing absolute position and orientation is difficult, e.g., in GPS-denied indoor environments [6]. In this paper, we study the problem of maintaining a triangular formation of three differential-drive robots using distance-based formation control.

Despite of the sensing advantage, distance-based formation control imposes a more stringent requirement on the interaction topology than the position- and displacement-based formation control. While the interaction graph does not have to be rigid for position- and displacement-based formation, graph rigidity is usually required for distance-based formation control [7]. Meanwhile, it is pointed out in [8] that while rigid formations are not globally stabilizable with gradient-descent control laws in general, rigid triangular formations can be stabilized with gradient-descent control laws. Indeed, [9] tackles the distance-based for-

The work was partially supported by the US National Science Foundation under grants CMMI#1825709 and IIS#1838799.

mation control problem of three single-integrator-modeled agents with a directed interaction graph. Inspired by [9], we present distance-based formation control for a three-robot system, and consider the kinematics of differential-drive robots and actuator saturation, and implement the distributed controllers in a robotic simulator.

In this paper, we first define the distance-based control problem for a system of three single-integrator modeled agents with an undirected interaction graph and a common desired velocity. We then present our main result that a rigid formation of three single-integrator modeled agents is stable under a distance-based control law if the initial locations of the three agents are non-collinear. Furthermore, we extend the results to a group of differential-drive mobile robots with actuator saturation nonlinearity. We evaluated the performance of the controller using a robot simulator V-REP.

The rest of the paper is organized as follows. In Section 2, we solve the formation control problem for a group of three single-integrator modeled agents. We then present the design of the controller for a group of differential drive robots in Section 3. In Section 4, we evaluate the control law using the robot simulator V-REP. Finally, the paper is concluded in Section 5.

2 Formation Control for Single-Integrator Modeled Agents

In this section, we first define the interaction topology for a group of three agents with the single-integrator model. Then the formation control problem is formulated, which is followed by a gradient-descent control law designed and proved.

2.1 Problem Statement

Suppose the motion of a group of three robots is governed by

$$\dot{\boldsymbol{p}}_i = \boldsymbol{v}_i, \quad i \in 1, 2, 3 \tag{1}$$

where $p_i = [x_i, \ y_i]^{\mathrm{T}} \in \mathbb{R}^2$ and $v_i = [v_{xi}, \ v_{yi}]^{\mathrm{T}} \in \mathbb{R}^2$ denote, respectively, the state and control of the i-th robot. The relative displacement \tilde{p}_{ij} of agent i with respect to agent j is defined as $\tilde{p}_{ij} = p_i - p_j$. Let \tilde{p} be the stack vector of \tilde{p}_{ij} , i.e., $\tilde{p} = [\tilde{p}_{12}^{\mathrm{T}}, \tilde{p}_{23}^{\mathrm{T}}, \tilde{p}_{31}^{\mathrm{T}}]^{\mathrm{T}} \in \mathcal{D}$, where \mathcal{D} is a manifold in \mathbb{R}^6 defined by

$$\mathcal{D} = \{ \tilde{\boldsymbol{p}} \in \mathbb{R}^6 : \, \tilde{\boldsymbol{p}}_{12} + \tilde{\boldsymbol{p}}_{23} + \tilde{\boldsymbol{p}}_{31} = \boldsymbol{0} \}$$
 (2)

The control objective is for the robots to achieve a desired formation and a desired velocity $\boldsymbol{v}^* = [v_x^*, v_y^*]^\mathrm{T} \in \mathbb{R}^2$. Given the desired distances $d_{ij}^* = d_{ji}^* \in (0, +\infty)$ for any $(i,j) \in \mathcal{E}^+$ where $\mathcal{E}^+ = \{(1,2),(2,3),(3,1)\}$, the desired formation is defined as

$$\mathcal{B} = \{ \tilde{\boldsymbol{p}} \in \mathcal{D} : ||\tilde{\boldsymbol{p}}_{ij}|| = d_{ij}^*, (i,j) \in \mathcal{E}^+ \}$$
 (3)

Note that the realizability [8] of the desired formation is ensured by the triangle inequality $d_{ij}^* < d_{ik}^* + d_{jk}^*$, for distinct $i, j, k \in \mathcal{V}$.

The interaction topology of the group of three robots can be modeled by a graph denoted $(\mathcal{V},\mathcal{E})$ where \mathcal{V} is the set of nodes, each corresponding to a robot, and $\mathcal{E} \subseteq \mathcal{V} \times \mathcal{V}$ is the set of edges (i,j). Each agent's accessibility to its neighbor's displacement is signified by the set of edges. Specifically, if an edge (i,j) exists from i to j, robot i has access to robot j's actual displacement \tilde{p}_{ji} relative to robot i and the desired distance d_{ij}^* from robot i at all times. The set of neighbors of the i-th robot is defined as $\mathcal{N}_i = \{j \in \mathcal{V} | (i,j) \in \mathcal{E}\}$. The Laplacian Matrix $\mathbf{L} = [l_{ij}] \in \mathbb{R}^{|\mathcal{V}| \times |\mathcal{V}|}$ of the graph is defined as

$$l_{ij} = \begin{cases} -1, & \text{if } i \neq j \land (i,j) \in \mathcal{E} \\ 0, & \text{if } i \neq j \land \neg (i,j) \in \mathcal{E} \\ \sum_{k \neq i} l_{ik}, & \text{if } i = j \end{cases}$$
 (4)

In our case, the vertex set is $\mathcal{V} = \{1,2,3\}$ and the edge set is $\mathcal{E} = \{(1,2),(1,3),(2,3),(2,1),(3,1),(3,2)\}$. We assume an undirected connected graph with the Laplacian matrix as:

$$\boldsymbol{L} = \begin{bmatrix} 2 & -1 & -1 \\ -1 & 2 & -1 \\ -1 & -1 & 2 \end{bmatrix} \tag{5}$$

Assumption 1 (Initial condition). *The initial positions of the robots are not collinear* [1,8]. *Namely,* $\tilde{\mathbf{p}}(0) \notin \mathcal{C}$, *where*

$$\mathcal{C} \triangleq \{ \tilde{\boldsymbol{p}} \in \mathcal{D} : \det[\tilde{\boldsymbol{p}}_{12}, \ \tilde{\boldsymbol{p}}_{23}] = 0 \}$$
 (6)

Let the formation separation error e_{ij} between agents i and j be defined as

$$e_{ij} = ||\tilde{\boldsymbol{p}}_{ij}|| - d_{ij}^*, \quad \forall (i,j) \in \mathcal{E}. \tag{7}$$

We define our distance-based formation control problem in the following.

Problem 1 (Single integrator). Given a three-agent system with Laplacian matrix (5), single-integrator model (1), and Assumption 1, find a control law v_i with $i \in V$ such that as $t \to \infty$, each robot reaches the desired velocity

$$\dot{\boldsymbol{p}}_i \to \boldsymbol{v}^*, \quad i \in \mathcal{V}.$$
 (8)

and the system achieves the desired formation \mathcal{B} , i.e.,

$$e_{ij} \to 0 \quad (i,j) \in \mathcal{E}$$
 (9)

2.2 Control Design

With a set of potential functions that take on their minimums at the desired distances, a gradient-descent control law can drive the system to its desired formation. A controller for single-integrator modeled agents can be written as

$$\boldsymbol{v}_i = \boldsymbol{v}^* - \nabla_{\boldsymbol{p}_i} \sum_{j \in \mathcal{N}_i} \gamma_{ij}(||\boldsymbol{p}_j - \boldsymbol{p}_i||^2), \quad (10)$$

where $\gamma_{ij}:(0,+\infty)\to\mathbb{R}$ is a differentiable potential function with only one minimum at d_{ij}^{*2} . We choose γ_{ij} as

$$\gamma_{ij}(||\boldsymbol{p}_j - \boldsymbol{p}_i||^2) = \frac{K}{2} \frac{(||\boldsymbol{p}_j - \boldsymbol{p}_i||^2 - d_{ij}^{*2})^2}{||\boldsymbol{p}_j - \boldsymbol{p}_i||^2}.$$
 (11)

where K > 0. Note that γ_{ij} quickly approaches infinity as $||\mathbf{p}_j - \mathbf{p}_i||^2 \to 0$. This property enables effective collision avoidance between neighboring robots.

Let $\beta_{ij}(\tilde{\boldsymbol{p}}) \triangleq ||\tilde{\boldsymbol{p}}_{ij}||^2 = ||\boldsymbol{p}_j - \boldsymbol{p}_i||^2$. The partial derivative of γ_{ij} with respect to β_{ij} can be written as

$$\rho_{ij} = \frac{\partial \gamma_{ij}(\beta_{ij})}{\partial \beta_{ij}} = \frac{K\left(\beta_{ij}^2 - d_{ij}^{*4}\right)}{\beta_{ij}^2}.$$
 (12)

The domain of definition of function ρ_{ij} is $\mathcal{D} \setminus \mathcal{Z}$ where $\mathcal{Z} = \mathcal{Z}_{12} \cup \mathcal{Z}_{23} \cup \mathcal{Z}_{31}$ and

$$\mathcal{Z}_{ij} = \{ \tilde{\boldsymbol{p}} \in \mathcal{D} : \ \tilde{\boldsymbol{p}}_{ij} = \boldsymbol{0} \}, \ (i,j) \in \mathcal{E}^+.$$

Then the controller (10) can be rewritten as

$$v_{i} = v^{*} - \sum_{j \in \mathcal{N}_{i}} \frac{\partial \gamma_{ij}(\beta_{ij})}{\partial \beta_{ij}} \frac{\partial \beta_{ij}}{\partial \mathbf{p}_{i}}$$

$$= v^{*} - \sum_{j \in \mathcal{N}_{i}} \rho_{ij} \cdot (\mathbf{p}_{i} - \mathbf{p}_{j})$$

$$= v^{*} - \sum_{j \in \mathcal{N}_{i}} \rho_{ij} \tilde{\mathbf{p}}_{ij}.$$
(13)

In view of (13), the system of inter-agent displacements can be written as

$$\dot{\tilde{p}} = \begin{bmatrix} \tilde{p}_{12} \\ \dot{\tilde{p}}_{23} \\ \dot{\tilde{p}}_{31} \end{bmatrix} = \begin{bmatrix} \dot{p}_{1} - \dot{p}_{2} \\ \dot{p}_{2} - \dot{p}_{3} \\ \dot{\tilde{p}}_{3} - \dot{p}_{1} \end{bmatrix} = \begin{bmatrix} v_{1} - v_{2} \\ v_{2} - v_{3} \\ v_{3} - v_{1} \end{bmatrix}
= - \begin{bmatrix} \rho_{12}\tilde{p}_{12} + \rho_{13}\tilde{p}_{13} - \rho_{21}\tilde{p}_{21} - \rho_{23}\tilde{p}_{23} \\ \rho_{21}\tilde{p}_{21} + \rho_{23}\tilde{p}_{23} - \rho_{31}\tilde{p}_{31} - \rho_{32}\tilde{p}_{32} \\ \rho_{31}\tilde{p}_{31} + \rho_{32}\tilde{p}_{32} - \rho_{12}\tilde{p}_{12} - \rho_{13}\tilde{p}_{13} \end{bmatrix}$$

$$= - \begin{bmatrix} \rho_{12}\tilde{p}_{12} - \rho_{31}\tilde{p}_{31} + \rho_{12}\tilde{p}_{12} - \rho_{23}\tilde{p}_{23} \\ -\rho_{12}\tilde{p}_{12} + \rho_{23}\tilde{p}_{23} - \rho_{31}\tilde{p}_{31} + \rho_{23}\tilde{p}_{23} \\ \rho_{31}\tilde{p}_{31} - \rho_{23}\tilde{p}_{23} - \rho_{12}\tilde{p}_{12} + \rho_{31}\tilde{p}_{31} \end{bmatrix}$$

$$= - \left(\begin{bmatrix} 2 & -1 & -1 \\ -1 & 2 & -1 \\ -1 & -1 & 2 \end{bmatrix} \otimes I_{2} \right) \begin{bmatrix} \rho_{12}\tilde{p}_{12} \\ \rho_{23}\tilde{p}_{23} \\ \rho_{31}\tilde{p}_{31} \end{bmatrix}$$

$$= -A\nu$$

where

$$m{A} riangleq m{L} \otimes m{I}_2 = egin{bmatrix} 2 & 0 & -1 & 0 & -1 & 0 \ 0 & 2 & 0 & -1 & 0 & -1 \ -1 & 0 & 2 & 0 & -1 & 0 \ 0 & -1 & 0 & 2 & 0 & -1 \ -1 & 0 & -1 & 0 & 2 & 0 \ 0 & -1 & 0 & -1 & 0 & 2 \end{pmatrix},$$

$$oldsymbol{
u} riangleq ((oldsymbol{W} \otimes oldsymbol{I}_2) ilde{oldsymbol{p}}) = egin{bmatrix}
ho_{12} ilde{oldsymbol{p}}_{12} \
ho_{23} ilde{oldsymbol{p}}_{23} \
ho_{31} ilde{oldsymbol{p}}_{31} \end{bmatrix} \in \mathbb{R}^6,$$

and

$$W = diag\{\rho_{12}, \rho_{23}, \rho_{31}\}$$

Note that (14) is not defined on \mathcal{Z} .

Lemma 1. $\dot{\tilde{p}} = 0$ if and only if $\rho_{12}\tilde{p}_{12} = \rho_{23}\tilde{p}_{23} = \rho_{31}\tilde{p}_{31}$.

Proof. Letting $\dot{\tilde{p}} = 0$ in (14) yields

$$A\nu = 0. (15)$$

We know that matrix A has an eigenvalue $\lambda_1 = 0$ with two eigenvectors ν_1 and ν_2 associated with it, where

$$m{
u}_1 = egin{bmatrix} 1 \ 0 \ 1 \ 0 \ 1 \ 0 \end{bmatrix}, \; m{
u}_2 = egin{bmatrix} 0 \ 1 \ 0 \ 1 \ 0 \ 1 \end{bmatrix}.$$

Hence the solution to (15) is $\nu = \alpha_1 \nu_1 + \alpha_2 \nu_2$ with $\alpha_1, \alpha_2 \in \mathbb{R}$, namely,

$$egin{bmatrix}
ho_{12} ilde{m{p}}_{12} \
ho_{23} ilde{m{p}}_{23} \
ho_{31} ilde{m{p}}_{31} \end{bmatrix} = egin{bmatrix} lpha_1 \ lpha_2 \ lpha_1 \ lpha_2 \end{bmatrix}.$$

Equivalently,

$$\rho_{12}\tilde{\boldsymbol{p}}_{12} = \rho_{23}\tilde{\boldsymbol{p}}_{23} = \rho_{31}\tilde{\boldsymbol{p}}_{31} = [\alpha_1, \, \alpha_2]^{\mathrm{T}}.$$

Let \mathcal{G} be a set of \tilde{p} in which $\dot{\tilde{p}} = 0$. From Lemma 1,

$$G = \{ \tilde{p} \in \mathcal{D} : \rho_{12} \tilde{p}_{12} = \rho_{23} \tilde{p}_{23} = \rho_{31} \tilde{p}_{31} \}.$$

Since $\rho_{12} = \rho_{23} = \rho_{31} = 0$ implies $\dot{\tilde{p}} = 0$, noticing (6), the set of desired equilibria \mathcal{B} is a proper subset of \mathcal{G} . Let $\mathcal{M} = \mathcal{G} \setminus \mathcal{B}$. In light of (3) and (12), we have

$$\mathcal{B} = \{ \tilde{\mathbf{p}} \in \mathcal{D} : \rho_{12} = \rho_{23} = \rho_{31} = 0 \}.$$

In view of (6), it follows that

$$\mathcal{M} = \mathcal{C} \cap \mathcal{G} = \mathcal{M}_0 \cup \mathcal{M}_1 \cup \mathcal{M}_2 \cup \mathcal{M}_3 \cup \mathcal{M}_4, \quad (16)$$

where

$$\mathcal{M}_{0} = (\mathcal{C} \cup \mathcal{G}) \setminus (\mathcal{Z}_{12} \cup \mathcal{Z}_{23} \cup \mathcal{Z}_{31}) = (\mathcal{C} \cup \mathcal{G}) \setminus \mathcal{Z}$$

$$\mathcal{M}_{1} = (\mathcal{C} \cup \mathcal{G}) \cap \mathcal{Z}_{12} \setminus (\mathcal{Z}_{23} \cup \mathcal{Z}_{31})$$

$$\mathcal{M}_{2} = (\mathcal{C} \cup \mathcal{G}) \cap \mathcal{Z}_{23} \setminus (\mathcal{Z}_{12} \cup \mathcal{Z}_{31})$$

$$\mathcal{M}_{3} = (\mathcal{C} \cup \mathcal{G}) \cap \mathcal{Z}_{31} \setminus (\mathcal{Z}_{12} \cup \mathcal{Z}_{23})$$

$$\mathcal{M}_{4} = \mathcal{Z}_{12} \cap \mathcal{Z}_{23} \cap \mathcal{Z}_{31}$$

We will show that trajectories starting outside of $\mathcal C$ are bounded away from $\mathcal M$. This can be achieved in several steps. As a first step, the following lemma shows that it holds within finite time.

Lemma 2. If $\tilde{\boldsymbol{p}}(0) \notin \mathcal{C}$, then $\tilde{\boldsymbol{p}}(t) \notin \mathcal{C}$ for $t < +\infty$.

Proof. For $p, q \in \mathbb{R}^2$, determinant $\det[p, q] = p^{\mathrm{T}}Gq$, where

$$\boldsymbol{G} = \begin{bmatrix} 0 & 1 \\ -1 & 0 \end{bmatrix}$$

In view of (2) and (14), it follows that

$$\frac{d}{dt} \det[\tilde{\boldsymbol{p}}_{12}, \ \tilde{\boldsymbol{p}}_{23}]
= \frac{d}{dt} \left(\tilde{\boldsymbol{p}}_{12}^{\mathrm{T}} \boldsymbol{G} \tilde{\boldsymbol{p}}_{23} \right) = \dot{\tilde{\boldsymbol{p}}}_{12}^{\mathrm{T}} \boldsymbol{G} \tilde{\boldsymbol{p}}_{23} + \tilde{\boldsymbol{p}}_{12}^{\mathrm{T}} \boldsymbol{G} \dot{\tilde{\boldsymbol{p}}}_{23}
= - \left(\rho_{12} \tilde{\boldsymbol{p}}_{12} - \rho_{31} \tilde{\boldsymbol{p}}_{31} + \rho_{12} \tilde{\boldsymbol{p}}_{12} - \rho_{23} \tilde{\boldsymbol{p}}_{23} \right)^{\mathrm{T}} \boldsymbol{G} \tilde{\boldsymbol{p}}_{23}
- \tilde{\boldsymbol{p}}_{12}^{\mathrm{T}} \boldsymbol{G} \left(-\rho_{12} \tilde{\boldsymbol{p}}_{12} + \rho_{23} \tilde{\boldsymbol{p}}_{23} - \rho_{31} \tilde{\boldsymbol{p}}_{31} + \rho_{23} \tilde{\boldsymbol{p}}_{23} \right)$$
(17)
$$= -\rho_{12} \tilde{\boldsymbol{p}}_{12}^{\mathrm{T}} \boldsymbol{G} \tilde{\boldsymbol{p}}_{23} + \rho_{31} \tilde{\boldsymbol{p}}_{31}^{\mathrm{T}} \boldsymbol{G} \tilde{\boldsymbol{p}}_{23} - \rho_{12} \tilde{\boldsymbol{p}}_{12}^{\mathrm{T}} \boldsymbol{G} \tilde{\boldsymbol{p}}_{23}
- \tilde{\boldsymbol{p}}_{12}^{\mathrm{T}} \boldsymbol{G} \rho_{23} \tilde{\boldsymbol{p}}_{23} + \tilde{\boldsymbol{p}}_{12}^{\mathrm{T}} \boldsymbol{G} \rho_{31} \tilde{\boldsymbol{p}}_{31} - \tilde{\boldsymbol{p}}_{12}^{\mathrm{T}} \boldsymbol{G} \rho_{23} \tilde{\boldsymbol{p}}_{23}
- \tilde{\boldsymbol{p}}_{12}^{\mathrm{T}} \boldsymbol{G} \rho_{23} \tilde{\boldsymbol{p}}_{23} + \tilde{\boldsymbol{p}}_{12}^{\mathrm{T}} \boldsymbol{G} \rho_{31} \tilde{\boldsymbol{p}}_{31} - \tilde{\boldsymbol{p}}_{12}^{\mathrm{T}} \boldsymbol{G} \rho_{23} \tilde{\boldsymbol{p}}_{23}
= -2 \left(\rho_{12} + \rho_{23} \right) \det[\tilde{\boldsymbol{p}}_{12}, \ \tilde{\boldsymbol{p}}_{23}]
+ \rho_{31} \left(\det[\tilde{\boldsymbol{p}}_{31}, \ \tilde{\boldsymbol{p}}_{23}] + \det[\tilde{\boldsymbol{p}}_{12}, \ \tilde{\boldsymbol{p}}_{31}] \right)
= -2 \left(\rho_{12} + \rho_{23} + \rho_{31} \right) \det[\tilde{\boldsymbol{p}}_{12}, \ \tilde{\boldsymbol{p}}_{23}]$$

Hence,

$$\det[\tilde{\boldsymbol{p}}_{12}(t), \ \tilde{\boldsymbol{p}}_{23}(t)] = \det[\tilde{\boldsymbol{p}}_{12}(0), \ \tilde{\boldsymbol{p}}_{23}(0)]e^{-2\int_0^t (\rho_{12}(z) + \rho_{23}(z) + \rho_{31}(z))dz}$$
(18)

Note that $\rho_{ij}(t) < K < +\infty$ for $(i,j) \in \mathcal{E}^+$ because of (12). Considering that $\tilde{p}(0) \notin \mathcal{C}$ is equivalent to $\det[\tilde{p}_{12}(0), \tilde{p}_{23}(0)] \neq 0$, we have, for $t < +\infty$, that

$$|\det[\tilde{\boldsymbol{p}}_{12}(t), \ \tilde{\boldsymbol{p}}_{23}(t)]| > |\det[\tilde{\boldsymbol{p}}_{12}(0), \ \tilde{\boldsymbol{p}}_{23}(0)]|e^{-2Kt} > 0.$$

Hence,
$$\tilde{\boldsymbol{p}}(t) \notin \mathcal{C}$$
 for $t < +\infty$.

In light of (16), $\mathcal{M} \subset \mathcal{C}$. Therefore, $\tilde{p}(t) \notin \mathcal{M}$ for $t < +\infty$. It remains to be shown that $\tilde{p}(t)$ will not enter \mathcal{M} as $t \to +\infty$, which will be done by proving Lemma 3 and Lemma 4. Let $\Theta : \mathcal{D} \setminus \mathcal{Z} \to \mathbb{R}$ be a function $\Theta(\tilde{p}) = \rho_{12}(\tilde{p}) + \rho_{23}(\tilde{p}) + \rho_{31}(\tilde{p})$.

Lemma 3. There exists an open set $W \subset \mathcal{D}$ such that $\mathcal{M} \subset W$ and for $\tilde{p} \in W \setminus \mathcal{Z}$, $\Theta(\tilde{p}) < 0$.

Proof. In (16), \mathcal{M} is divided into 5 subsets. Note that $\Theta(\tilde{p})$ is defined on \mathcal{M}_0 , but not on \mathcal{M}_1 , \mathcal{M}_2 , \mathcal{M}_3 , or \mathcal{M}_4 . Before proceeding, let

$$\mathcal{W}_i(\epsilon) \triangleq \{ \tilde{m{p}} \in \mathcal{D} : \inf_{m{m} \in \mathcal{M}_i} || \tilde{m{p}} - m{m} || < \epsilon \}.$$

First let's suppose $\tilde{p} \in \mathcal{M}_0$. Since $\mathcal{M}_0 \subset \mathcal{G}$, we have $\rho_{12}\tilde{p}_{12} = \rho_{23}\tilde{p}_{23} = \rho_{31}\tilde{p}_{31}$. Since $\mathcal{M}_0 \subset \mathcal{C}$, we have $||\tilde{p}_{ij}|| = ||\tilde{p}_{jk}|| + ||\tilde{p}_{ki}||$ for distinct $i, j, k \in \mathcal{V}$. Without loss of generality, suppose

$$||\tilde{\boldsymbol{p}}_{12}|| = ||\tilde{\boldsymbol{p}}_{23}|| + ||\tilde{\boldsymbol{p}}_{31}||.$$
 (19)

Because $\mathcal{M}_0\subset\mathcal{C}$ means $\tilde{p}_{12},\,\tilde{p}_{23}$ and \tilde{p}_{31} are collinear, we have

$$\rho_{12}||\tilde{\boldsymbol{p}}_{12}|| = -\rho_{23}||\tilde{\boldsymbol{p}}_{23}|| = -\rho_{31}||\tilde{\boldsymbol{p}}_{31}||.$$
(20)

Now we will prove $\rho_{12}>0$ by contradiction. Since $\mathcal{M}_0\cap\mathcal{Z}=\emptyset$, we have $\rho_{12},\rho_{23},\rho_{31}\neq0$. Suppose $\rho_{12}<0$. With (20), it follows that $\rho_{23}>0$ and $\rho_{31}>0$. Considering (12), we have $||\tilde{\boldsymbol{p}}_{12}||< d_{12}^*, ||\tilde{\boldsymbol{p}}_{23}||> d_{23}^*$ and $||\tilde{\boldsymbol{p}}_{31}||> d_{31}^*$. As the triangular inequality must be satisfied for d_{12}^* , d_{23}^* and d_{31}^* , we have

$$0 < d_{23}^* + d_{31}^* - d_{12}^* < ||\tilde{p}_{23}|| + ||\tilde{p}_{31}|| - ||\tilde{p}_{12}||$$

This is in contradiction with (19). Hence, $\rho_{12} > 0$. In light of (19) and (20), we have

$$\begin{split} \Theta(\tilde{\boldsymbol{p}}) &= \rho_{12} + \rho_{23} + \rho_{31} \\ &= \rho_{12} - \frac{||\tilde{\boldsymbol{p}}_{12}||}{||\tilde{\boldsymbol{p}}_{23}||} \rho_{12} - \frac{||\tilde{\boldsymbol{p}}_{12}||}{||\tilde{\boldsymbol{p}}_{31}||} \rho_{12} \\ &= \rho_{12} \left(1 - \frac{||\tilde{\boldsymbol{p}}_{12}||}{||\tilde{\boldsymbol{p}}_{23}||} - \frac{||\tilde{\boldsymbol{p}}_{12}||}{||\tilde{\boldsymbol{p}}_{31}||} \right) < 0 \end{split}$$

Since ρ_{ij} is locally Lipschitz, there must exist an $\epsilon_0 > 0$ such that if $\tilde{\boldsymbol{p}} \in \mathcal{W}_0(\epsilon_0)$, then $\Theta(\tilde{\boldsymbol{p}}) < 0$.

Next let's analyze the value of $\Theta(\cdot)$ in the neighborhood of \mathcal{M}_1 , \mathcal{M}_2 and \mathcal{M}_3 . Observing (12), we find ρ_{ij} is bounded above by K, but does not have a lower bound. Let $\epsilon_1 = 3^{-1/4} \cdot d_{12}^*$. Suppose $\tilde{p} \in \mathcal{W}_1(\epsilon_1) \setminus \mathcal{Z}$. Since $\mathcal{M}_1 \subset \mathcal{Z}_{12}$, we have $||\tilde{p}_{12}|| < \epsilon_1$. In view of (12), we find

$$\rho_{12} < \frac{K\left(\epsilon_1^4 - d_{12}^{*4}\right)}{\epsilon_1^4} < -2K.$$

Since ρ_{23} , $\rho_{31} < K$, it follows that $\Theta(\cdot) < 0$. In summary, $\Theta(\tilde{\boldsymbol{p}}) < 0$ on $\mathcal{W}_1(\epsilon_1) \setminus \mathcal{Z}$. The same reasoning can be used to show $\Theta(\cdot) < 0$ on both $\mathcal{W}_2(\epsilon_2) \setminus \mathcal{Z}$ and $\mathcal{W}_3(\epsilon_3) \setminus \mathcal{Z}$, where $\epsilon_2 = 3^{-1/4} \cdot d_{23}^*$ and $\epsilon_3 = 3^{-1/4} \cdot d_{31}^*$.

Finally, it is obvious that $\Theta(\cdot) < 0$ on $\mathcal{W}_4(\epsilon_4) \setminus \mathcal{Z}$ where $\epsilon_4 = \min\{d_{12}^*, d_{23}^*, d_{31}^*\}.$

Let

$$W = \bigcup_{i=0}^{4} W_i(\epsilon_i). \tag{21}$$

Since $\mathcal{M}_i \subset \mathcal{W}_i(\epsilon_i)$, we have

$$\mathcal{M} = \bigcup_{i=0}^4 \mathcal{M}_i \subset \bigcup_{i=0}^4 \mathcal{W}_i(\epsilon_i) = \mathcal{W}.$$

In conclusion, there exists an open set W such that $\mathcal{M} \subset \mathcal{W}$ and for $\tilde{p} \in \mathcal{W} \setminus \mathcal{Z}$, $\Theta(\tilde{p}) < 0$.

Lemma 4. If the initial positions of the robots are not collinear, then the trajectories of system (1) with Laplacian matrix (5) driven by control law (13) will not approach M as $t \to \infty$.

Proof. We will prove this by contradiction. Suppose the opposite is true. That is, there exists a trajectory $\tilde{\boldsymbol{p}}(t)$ such that $\tilde{\boldsymbol{p}}(0) \in \mathcal{D} \setminus \mathcal{C}$ and $\tilde{\boldsymbol{p}}(t)$ tends to \mathcal{M} as $t \to +\infty$. Since $\mathcal{M} \subset \mathcal{C}$, we have

$$\lim_{t \to \infty} \det[\tilde{\mathbf{p}}_{12}(t), \ \tilde{\mathbf{p}}_{23}(t)] = 0. \tag{22}$$

Let \mathcal{W} be the open set in (21). Since $\mathcal{W} \supset \mathcal{M}$ and $\tilde{p}(t)$ tends to \mathcal{M} as $t \to +\infty$, there must exist a time $T \in (0, +\infty)$ such that $\tilde{p}(t) \in \mathcal{W}$ for $t \in [T, +\infty)$. According to Lemma 2, $\tilde{p}(T) \notin \mathcal{C}$ because $T < +\infty$. Hence,

$$\det[\tilde{p}_{12}(T), \ \tilde{p}_{23}(T)] > 0.$$

From (17), we can obtain that, for t > T,

$$\det[\tilde{\boldsymbol{p}}_{12}(t), \ \tilde{\boldsymbol{p}}_{23}(t)]$$

$$= \det[\tilde{\boldsymbol{p}}_{12}(T), \ \tilde{\boldsymbol{p}}_{23}(T)]e^{-2\int_{T}^{t}(\rho_{12}(z)+\rho_{23}(z)+\rho_{31}(z))dz}$$

$$= \det[\tilde{\boldsymbol{p}}_{12}(T), \ \tilde{\boldsymbol{p}}_{23}(T)]e^{-2\int_{T}^{t}(\Theta(\tilde{\boldsymbol{p}}(z)))dz}$$

$$> \det[\tilde{\boldsymbol{p}}_{12}(T), \ \tilde{\boldsymbol{p}}_{23}(T)] > 0.$$
(23)

As $t \to +\infty$, (23) is in contradiction with (22). Therefore, all trajectories starting outside \mathcal{C} will not approach \mathcal{M} even if $t \to +\infty$.

Proposition 1 (Single integrator). Consider system (1) with Laplacian matrix (5), driven by control law (13). If Assumption 1 is satisfied, then $\lim_{t\to\infty} e_{ij}(t) = 0$ for $(i,j) \in \mathcal{E}$ and $\lim_{t\to\infty} \dot{\mathbf{p}}_i = \mathbf{v}^*$ for $i \in \mathcal{V}$. That is, Problem 1 is solved by the controller (13).

Proof. Consider the candidate Lyapunov function

$$V(\tilde{\boldsymbol{p}}) = \gamma_{12}(\beta_{12}(\tilde{\boldsymbol{p}})) + \gamma_{23}(\beta_{23}(\tilde{\boldsymbol{p}})) + \gamma_{31}(\beta_{31}(\tilde{\boldsymbol{p}}))$$

$$= \sum_{(i,j)\in\mathcal{E}^+} \gamma_{ij}(\beta_{ij}(\tilde{\boldsymbol{p}}))$$

$$= \sum_{(i,j)\in\mathcal{E}^+} \frac{(\beta_{ij}(\tilde{\boldsymbol{p}}) - d_{ij}^{*2})^2}{\beta_{ij}(\tilde{\boldsymbol{p}})}.$$

Obviously, we have

$$\begin{cases} V(\tilde{\boldsymbol{p}}) = 0, & \forall \tilde{\boldsymbol{p}} \in \mathcal{B}; \\ V(\tilde{\boldsymbol{p}}) > 0, & \text{otherwise.} \end{cases}$$

Since

$$\dot{\beta}_{ij}(\tilde{\boldsymbol{p}}) = \frac{d}{dt} ||\tilde{\boldsymbol{p}}_{ij}||^2 = 2\tilde{\boldsymbol{p}}_{ij}^{\mathrm{T}} \dot{\tilde{\boldsymbol{p}}}_{ij},$$

The derivative of the candidate Lyapunov functioncan be

derived as

$$\dot{V}(\tilde{p}) = \frac{\partial V}{\partial \beta_{12}} \dot{\beta}_{12} + \frac{\partial V}{\partial \beta_{23}} \dot{\beta}_{23} + \frac{\partial V}{\partial \beta_{31}} \dot{\beta}_{31}
= \frac{\partial \gamma_{12}(\beta_{12})}{\partial \beta_{12}} \dot{\beta}_{12} + \frac{\partial \gamma_{23}(\beta_{23})}{\partial \beta_{23}} \dot{\beta}_{23} + \frac{\partial \gamma_{31}(\beta_{31})}{\partial \beta_{31}} \dot{\beta}_{31}
= \rho_{12} \dot{\beta}_{12} + \rho_{23} \dot{\beta}_{23} + \rho_{31} \dot{\beta}_{31}
= 2\rho_{12} \tilde{p}_{12}^{\mathrm{T}} \dot{\tilde{p}}_{12} + 2\rho_{23} \tilde{p}_{23}^{\mathrm{T}} \dot{\tilde{p}}_{23} + 2\rho_{31} \tilde{p}_{31}^{\mathrm{T}} \dot{\tilde{p}}_{31}
= 2 \cdot \begin{bmatrix} \rho_{12} \tilde{p}_{12} \\ \rho_{23} \tilde{p}_{23} \\ \rho_{31} \tilde{p}_{31} \end{bmatrix}^{\mathrm{T}} \begin{bmatrix} \dot{\tilde{p}}_{12} \\ \dot{\tilde{p}}_{23} \\ \dot{\tilde{p}}_{31} \end{bmatrix}
= -2 \nu^{\mathrm{T}} A \nu.$$

Since A is positive semidefinite and K is a positive number, we have

$$\begin{cases} \dot{V}(\tilde{\boldsymbol{p}}) = 0, & \forall \tilde{\boldsymbol{p}} \in \mathcal{B}; \\ \dot{V}(\tilde{\boldsymbol{p}}) \leq 0, & \text{otherwise}. \end{cases}$$

Letting $\dot{V}(\tilde{\boldsymbol{p}}) = 0$ yields

$$\boldsymbol{\nu}^{\mathrm{T}} \boldsymbol{A} \boldsymbol{\nu} = 0 \tag{24}$$

Using eigendecomposition, A can be factorized as

$$A = Q\Lambda Q^{-1}$$

where $\Lambda = diag\{0, 0, 3, 3, 3, 3\}$, and

$$\boldsymbol{Q} = \begin{bmatrix} \frac{\sqrt{3}}{3} & 0 & -\frac{\sqrt{2}}{2} & 0 & -\frac{\sqrt{2}\sqrt{3}}{6} & 0\\ 0 & \frac{\sqrt{3}}{3} & 0 & -\frac{\sqrt{2}}{2} & 0 & -\frac{\sqrt{2}\sqrt{3}}{6} \\ \frac{\sqrt{3}}{3} & 0 & \frac{\sqrt{2}}{2} & 0 & -\frac{\sqrt{2}\sqrt{3}}{6} & 0\\ 0 & \frac{\sqrt{3}}{3} & 0 & \frac{\sqrt{2}}{2} & 0 & -\frac{\sqrt{2}\sqrt{3}}{6} \\ \frac{\sqrt{3}}{3} & 0 & 0 & 0 & \frac{\sqrt{2}\sqrt{3}}{3} & 0\\ 0 & \frac{\sqrt{3}}{3} & 0 & 0 & 0 & \frac{\sqrt{2}\sqrt{3}}{3} \end{bmatrix}$$

is an orthogonal matrix.

Then Eqn. (24) can be rewritten as

$$0 = \boldsymbol{\nu}^{\mathrm{T}} \boldsymbol{A} \boldsymbol{\nu} = \boldsymbol{\nu}^{\mathrm{T}} \boldsymbol{Q} \boldsymbol{\Lambda} \boldsymbol{Q}^{-1} \boldsymbol{\nu}$$
$$= \left(\boldsymbol{Q}^{\mathrm{T}} \boldsymbol{\nu} \right)^{\mathrm{T}} \boldsymbol{\Lambda} \left(\boldsymbol{Q}^{\mathrm{T}} \boldsymbol{\nu} \right).$$

It follows that

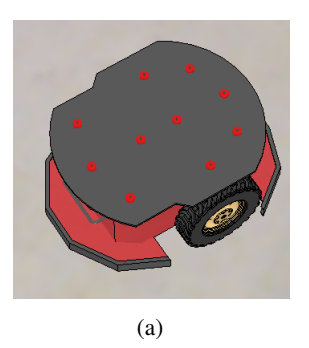
$$\boldsymbol{Q}^{\mathrm{T}}\boldsymbol{\nu} = [\sqrt{3}\alpha_{1}, \sqrt{3}\alpha_{2}, 0, 0, 0, 0]^{\mathrm{T}}$$

for some $\alpha_1, \alpha_2 \in \mathbb{R}$. Hence,

$$\begin{bmatrix} \rho_{12}\tilde{\boldsymbol{p}}_{12} \\ \rho_{23}\tilde{\boldsymbol{p}}_{23} \\ \rho_{31}\tilde{\boldsymbol{p}}_{31} \end{bmatrix} = \boldsymbol{\nu} = \boldsymbol{Q} \begin{bmatrix} \sqrt{3}\alpha_1 \\ \sqrt{3}\alpha_2 \\ 0 \\ 0 \\ 0 \end{bmatrix} = \begin{bmatrix} \alpha_1 \\ \alpha_2 \\ \alpha_1 \\ \alpha_2 \\ \alpha_1 \\ \alpha_2 \end{bmatrix}.$$

Equivalently, $\tilde{p} \in \mathcal{G}$. By Lemma 2 and Lemma 4, it follows that $\tilde{p} \in \mathcal{B}$. Thus by Lasalle's Invariance Principle, we can conclude that \mathcal{B} is asymptotically stable. Therefore, $\lim_{t\to\infty} e_{ij}(t) = 0$ for $(i,j) \in \mathcal{E}$.

Since $\lim_{t\to\infty} e_{ij}(t) = 0$, the second term of the control law (13) also tends to 0. It follows that $\lim_{t\to\infty} \dot{p}_i = v^*$ for $i \in \mathcal{V}$.



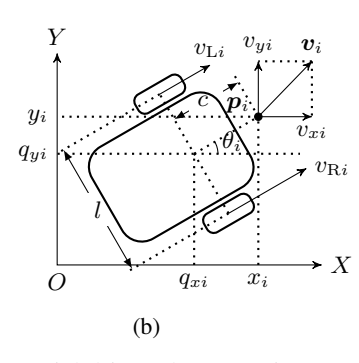


Figure 1: Kinematics of a differential drive robot. (a) Pioneer P3-DX robot; (b) Schematic illustration.

3 Formation Control for Differential Drive Robots

In this section, we first present the kinematic model of a group of differential drive robots. Then the controller discussed in Section 2 is generalized to control this nonholonomic multi-robot system.

3.1 Differential drive robot kinematics

Pioneer P3-Dx, a two-wheel differential drive robot, is considered in this paper. Assuming that it moves only on a planer surface, its state equation can be expressed as

$$\dot{\boldsymbol{q}}_i = \boldsymbol{G}(\boldsymbol{q}_i) \operatorname{sat}_{v_{\mathrm{m}}} (\boldsymbol{\Gamma}_i), \quad i = 1, 2, 3,$$
 (25)

where the *i*-th robot's pose $\mathbf{q}_i = [q_{xi}, q_{yi}, \theta_i]^{\mathrm{T}} \in SE(2)$ consists of the displacement $[q_{xi}, q_{yi}]^{\mathrm{T}} \in \mathbb{R}^2$ of the midpoint of the line segment connecting the robot's two driving wheels and the orientation $\theta_i \in SO(2)$ of the robot. The matrix $\mathbf{G}(\mathbf{q}_i)$ is written as

$$m{G}(m{q}_i) = egin{bmatrix} rac{\cos heta_i}{2} & rac{\cos heta_i}{2} \ rac{\sin heta_i}{2} & rac{\sin heta_i}{2} \ -rac{1}{l} & rac{1}{l} \ \end{pmatrix},$$

where l is the distance between the two driving wheels. The control input $\Gamma_i = [v_{\mathrm{L}i}, v_{\mathrm{R}i}]^\mathrm{T} \in \mathbb{R}^2$ represents the wheel velocity input, which is comprised of the left wheel linear speed $v_{\mathrm{L}i}$ and the right wheel linear speed $v_{\mathrm{R}i}$ of the i-th robot. The saturation function $\mathbf{sat}_{v_{\mathrm{m}}}: \mathbb{R}^2 \to [-v_{\mathrm{m}}, v_{\mathrm{m}}]^2$ is defined as

$$\mathbf{sat}_{v_{\mathrm{m}}}\left(\mathbf{\Gamma}_{i}
ight) = egin{bmatrix} \mathrm{sat}_{v_{\mathrm{m}}}\left(v_{\mathrm{L}i}
ight) \ \mathrm{sat}_{v_{\mathrm{m}}}\left(v_{\mathrm{R}i}
ight) \end{bmatrix}$$

where $\text{sat}_{v_{\text{m}}}(v) \triangleq \text{sgn}(v) \cdot \min\{v_{\text{m}}, |v|\}$ and , and v_m is the maximum speed limit.

3.2 Coordinate Transformation

As shown in Fig.1b, we define a reference point located at $p_i = [x_i, y_i]$. If we set c = l/2, the nonholonomic kinematic model (25) can be converted to the single-integrator model (1). That is, in the new coordinate defined by

$$\begin{bmatrix} x_i \\ y_i \end{bmatrix} = \begin{bmatrix} q_{xi} + c\cos\theta_i \\ q_{ui} + c\sin\theta_i \end{bmatrix},\tag{26}$$

we can derive the robot model as [10]

$$\begin{bmatrix} \dot{x}_i \\ \dot{y}_i \end{bmatrix} = \begin{bmatrix} v_{xi} \\ v_{yi} \end{bmatrix}. \tag{27}$$

Control input $\Gamma_i' \in \mathbb{R}^2$ is defined as

$$\Gamma_{i}' \triangleq \begin{bmatrix} v_{\text{L}i}' \\ v_{\text{R}i}' \end{bmatrix} \\
= \begin{bmatrix} \sin \theta_{i} + \frac{l}{2c} \cos \theta_{i} & \sin \theta_{i} - \frac{l}{2c} \cos \theta_{i} \\ -\sin \theta_{i} + \frac{l}{2c} \cos \theta_{i} & \sin \theta_{i} + \frac{l}{2c} \cos \theta_{i} \end{bmatrix} \begin{bmatrix} v_{xi} \\ v_{yi} \end{bmatrix}.$$
(28)

After the coordinate transformation, we can apply the control law (13) to the single-integrator model based on Proposition 1.

3.3 Actuator Saturation Nonlinearity

For Pioneer robots, the maximum speed of each wheel/actuator is limited to v_m in (25). The velocity generated by the robot controller needs to undergo the following transformation before being input to the actuators

$$\begin{bmatrix} v_{\mathrm{L}i} \\ v_{\mathrm{R}i} \end{bmatrix} = \min \left\{ v_m, \frac{v_m}{\max\{|v'_{\mathrm{L}i}|, |v'_{\mathrm{R}i}|\}} \right\} \cdot \begin{bmatrix} v'_{\mathrm{L}i} \\ v'_{\mathrm{R}i} \end{bmatrix} \quad (29)$$

Here we prove that the trajectory of a robot will not be changed by this transformation.

We omit the subscript i in the following proof. The curvature of the trajectory is defined as

$$R \triangleq \frac{ds}{d\theta} = \frac{ds}{dt} \left(\frac{d\theta}{dt}\right)^{-1}$$

where

$$ds \triangleq \sqrt{dx^2 + dy^2}.$$

Since

$$\frac{d\theta}{dt} = \frac{v_{\rm L} - v_{\rm R}}{l},$$

we find that, before the transformation, the radius of curvature of the trajectory is

$$R' = \frac{2(v'_{\rm L} - v'_{\rm R})}{l(v'_{\rm I} + v'_{\rm R})}.$$

After the transformation, the radius of curvature of the trajectory is

$$R = \frac{2(v_{\rm L} - v_{\rm R})}{l(v_{\rm L} + v_{\rm R})}.$$
 (30)

Substituting the transformation (29) into (30), it can be seen that

$$R' = R, \quad \forall v_{\rm L}, v_{\rm R}$$

Hence, the radius of curvature is preserved by this transformation. Thus, the trajectory is not changed by applying (29).

The control procedure for each differential-drive robot (25) is summarized in Algorithm 1.

Algorithm 1 The control algorithm for the *i*-th robot

Input: The relative displacements \tilde{p}_{ij} of robot i from robots j, $j \in \mathcal{N}_i$, pose q_i of robot i, and the desired velocity v^* .

Output: The wheel velocities Γ_i .

- 1: Calculate the control input for the single-integrator model $v_i \leftarrow \text{Substitute } v^* \text{ and } \tilde{p}_{ij}, j \in \mathcal{N}_i, \text{ into (13)}$
- 2: Apply the input transformation to obtain the wheel velocities $\Gamma'_i \leftarrow$ Substitute v_i and q_i into (28)
- 3: Scale down the wheel velocities $\Gamma_i \leftarrow \text{Substitute } \Gamma_i \text{ into (29)}$

4 Simulation

In this section, we demonstrate the performance of the designed controller in a robot simulator.

4.1 Experiment Setup

A robot simulator V-REP [11] is used to evaluate the performance of the controller. In V-REP, Bullet Physics Library makes the robot dynamics calculation realistic as the physical robot platform. The simulation scenario, containing three P3-DX robots on a flat floor without obstacles, is shown in Fig. 2. Each driving wheel motor of the robot is configured to be capable of producing 3N·m of torque, while the maximum linear speed of the driving wheels are limited to 0.7 m/s.

The controller is implemented in Python as a remote API client that operates in synchronization with the simulation loop which runs at 20Hz. The velocity from the controller is input to the robot motors while a built-in low-level controller calculates the torque to be applied to each wheel based on the difference between the target and actual wheel velocities.

4.2 Simulation Results

We evaluate the performance of the control law summarized in the stepwise procedure described in Section 3.3. The setup of the simulation is described as follows. The desired formation is set to $d_{12}^*=1$ m, $d_{23}^*=2$ m, and $d_{31}^*=\sqrt{3}$ m. The maximum wheel linear speed is $v_{\rm m}=0.7$ m/s. The common desired velocity is ${\pmb v}^*=[0.25,0.5\sqrt{3}]$ (m/s). The controller parameter is chosen as K=0.15.

Simulation results are shown in Fig. 2 and Fig. 3. It can be seen that the formation separation errors reduce from 4m to 0 within 7 seconds. The robot wheel velocities initially are maxed at 0.7m/s and then settled to the common desired velocity 0.5m/s. Fig. 3b shows the trajectories of the three robots that achieve the triangular formation and then move in consensus at the desired velocity.

5 Conclusion

In this paper, we designed a distance-based formation control law for a group of three differential-drive robots. Specifically, we applied a coordinate transformation technique to convert the nonholonomic robot kinematic model to a single-integrator model. Then a gradient-descent control law was employed to stabilize the formation of the single-integrator modeled robot system. The actuator input saturation nonlinearity was also considered. Finally, the

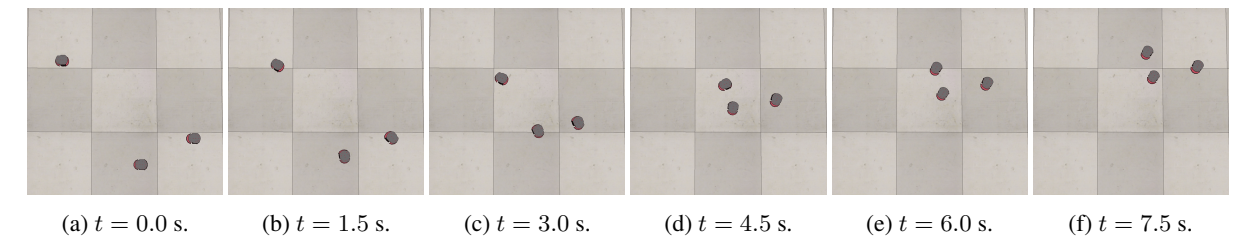


Figure 2: Snapshots of the simulation scenario in V-REP robot simulator.

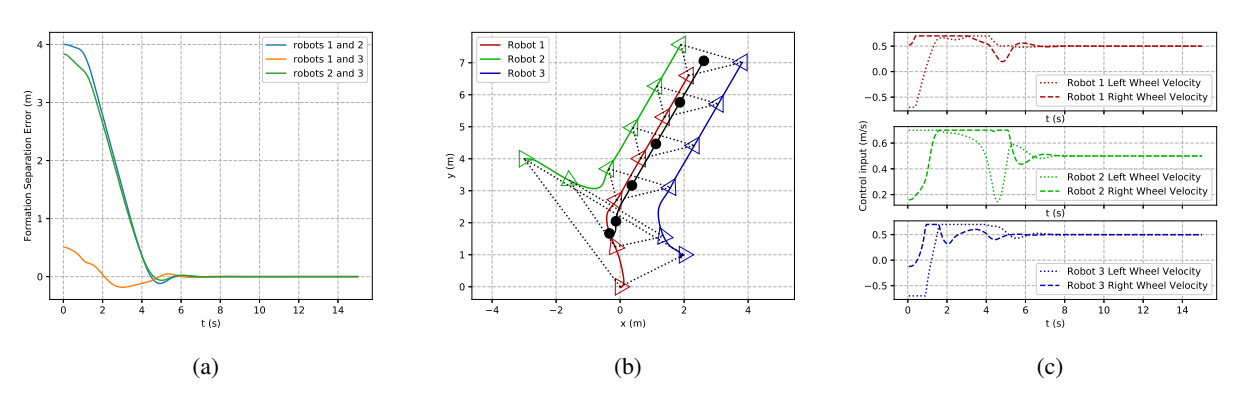


Figure 3: Performance of the proposed control law. (a) Formation separation error $e_{ij}(t)$. (b) Trajectories of the three robots are denoted by solid curves in red, green and blue. Triangles represent the pose of the robots every 3 seconds. Solid circles and black curves illustrate the trajectory of their center of mass. (c) Robot control input $[v_{Li}, v_{Ri}]^T$.

performance of the control law was evaluated using a robot simulator V-REP. In the future work, we plan to extend the three-robot system control to a larger group of robots consisting of triangular structures.

REFERENCES

- K.-K. Oh, M.-C. Park, and H.-S. Ahn, "A survey of multiagent formation control," *Automatica*, vol. 53, pp. 424

 –440, 2015.
- [2] A. K. Das, R. Fierro, V. Kumar, J. P. Ostrowski, J. Spletzer, and C. J. Taylor, "A vision-based formation control framework," *IEEE Transactions on Robotics and Automation*, vol. 18, pp. 813–825, 2002.
- [3] P. Vela, A. Betser, J. Malcolm, and A. Tannenbaum, "Vision-based range regulation of a leader-follower formation," *IEEE Transactions on Control Systems Technology*, vol. 17, no. 2, pp. 442–448, 2009.
- [4] N. Moshtagh, N. Michael, A. Jadbabaie, and K. Daniilidis, "Vision-based, distributed control laws for motion coordination of nonholonomic robots," *IEEE Transactions on Robotics*, vol. 25, no. 4, pp. 851–860, 2009.
- [5] D. Guo, H. Wang, W. Chen, M. Liu, Z. Xia, and K. K. Leang, "A unified leader-follower scheme for mobile robots with uncalibrated on-board camera," in *IEEE International Conference on Robotics and Automation*, pp. 3792–3797, 2017.
- [6] M. Saska, T. Baca, J. Thomas, J. Chudoba, L. Preucil, T. Krajnik, J. Faigl, G. Loianno, and V. Kumar, "System for deployment of groups of unmanned micro aerial vehicles in GPS-denied environments using onboard visual relative localization," *Autonomous Robots*, vol. 41, no. 4, pp. 919– 944, 2017.
- [7] D. V. Dimarogonas and K. H. Johansson, "On the stability of distance-based formation control," in *IEEE Conference*

- on Decision and Control, pp. 1200-1205, 2008.
- [8] K.-K. Oh and H.-S. Ahn, "Formation control of mobile agents based on inter-agent distance dynamics," *Automatica*, vol. 47, no. 10, pp. 2306–2312, 2011.
- [9] B. Anderson, M. Cao, S. Dasgupta, A. Morse, and C. Yu, "Maintaining a directed, triangular formation of mobile autonomous agents," *Communications in Information and Systems*, vol. 11, no. 1, pp. 1–16, 2011.
- [10] S. Li, R. Kong, and Y. Guo, "Cooperative distributed source seeking by multiple robots: Algorithms and experiments," *IEEE/ASME Transactions on mechatronics*, vol. 19, no. 6, pp. 1810–1820, 2014.
- [11] E. Rohmer, S. P. Singh, and M. Freese, "V-rep: A versatile and scalable robot simulation framework," in *IEEE/RSJ In*ternational Conference on Intelligent Robots and Systems, pp. 1321–1326, 2013.